$St(Re_x)^{1/2}$ and friction group $(c_f/2)(Re_x)^{1/2}$ for $\omega = 0.75$ was less than the predicted values for $\omega = 1$ by 12% (at $g_w = 2$, the difference is less, being 4–5%). The effect of flow speed (compressibility) is well known for the case of constant free-stream velocity ($\bar{\beta} = 0$); e.g., from Crocco's calculations (e.g., see Ref. 10) at a Mach number of 5 for $\gamma = 1.4$ ($S = 0.83$) and $Pr = 0.725$, values of the friction group for $\omega = 0.75$ are below the values for $\omega = 1.0$ by 16% for an adiabatic surface and by 10% for the highest temperature surface considered, $g_w = 2$. At a sonic condition $M_e = 1$, $S = 0.17$, the respective differences are less, being lower by 1% and 5%, the latter of which is essentially the same as the low-speed value previously mentioned. Similar remarks apply to the heat-transfer group. The magnitude of these differences cited might also be found in accelerated flows by inference from recent similarity calculations in Ref. 11, which, however, were carried out for wall cooling. It would appear that differences from the values for the heat transfer and friction relations given by Eqs. (5) and (4) would be relatively small for channel flows, for example, for hydrogen and helium ($\omega \simeq 0.7$) at flow speeds less than sonic ($S \leq 0.17$ and 0.25, respectively).

IV. Concluding Remarks

The effect of large wall heating and flow acceleration on the structure of laminar boundary layers was investigated over a range of flow speeds. The heat-transfer parameter G_w' was found to increase significantly with the amount of wall heating in flow acceleration regions. This trend suggests taking advantage of heating in flow acceleration regions provided that frictional effects are not important and that the laminar boundary layer is not on the verge of transition to a turbulent boundary layer before the flow is accelerated. Because of flow acceleration the velocity profiles with wall heating do not have an inflection point in the region near the wall where the velocity increases and therefore would appear to be more stable to small disturbances. This view is supported by other observations on laminarization of turbulent flows through circular tubes,[12,13] where flow acceleration occurred because of energy transfer from the heated wall.

References

[1] Cohen, C. B. and Reshotko, E., "Similar Solutions for the Compressible Laminar Boundary Layer With Heat Transfer and Pressure Gradient," R-1293, 1956, NACA.

[2] Back, L. H. and Witte, A. B., "Prediction of Heat Transfer From Laminar Boundary Layers, With Emphasis on Large Free-Stream Velocity Gradients and Highly Cooled Walls," *Transactions of the ASME, Ser. C: Journal of Heat Transfer*, Vol. 88, Aug. 1966, pp. 249–256.

[3] Back, L. H., "Effects of Severe Surface Cooling and Heating on the Structure of Low-Speed, Laminar Boundary-Layer Gas Flows with Constant Free-Stream Velocity," TR 32-1301, 1968, Jet Propulsion Lab., Pasadena, Calif.

[4] Van Driest, E. R., "Investigation of Laminar Boundary Layer in Compressible Fluids Using the Crocco Method," TN 2597, Jan. 1952, NACA.

[5] Mirels, H. and Welsh, W. E., Jr., "Stagnation-Point Boundary Layer with Large Wall-to-Freestream Enthalpy Ratio," *AIAA Journal*, Vol. 6, No. 6, June 1968, pp. 1105–1111.

[6] Back, L. H., "Acceleration and Cooling Effects in Laminar Boundary Layers—Subsonic, Transonic and Supersonic Speeds," *AIAA Journal*, Vol. 8, No. 4, April 1970, pp. 794–802.

[7] Back, L. H., "Flow and Heat Transfer in Laminar Boundary Layers With Swirl," *AIAA Journal*, Vol. 7, No. 9, Sept. 1969, pp. 1781–1789.

[8] Lees, L., "Laminar Heat Transfer Over Blunt-Nosed Bodies at Hypersonic Flight Speeds," *Jet Propulsion*, Vol. 26, 1956, pp. 259–269.

[9] Marvin, J. G. and Sinclair, A. R., "Convective Heating in Regions of Large Favorable Pressure Gradient," *AIAA Journal*, Vol. 5, Nov. 1967, pp. 1940–1948.

[10] Howarth, L., *Modern Developments in Fluid Dynamics—High Speed Flow*, Oxford University Press, London, 1953.

[11] Wortman, A. and Mills, A. F., "Highly Accelerated Compressible Laminar Boundary Layer Flows with Mass Transfer," ASME Paper 70-HT/SPT-34, June 1970; *Transactions of the ASME, Ser. C: Journal of Heat Transfer*, to be published.

[12] Bankston, C. A., "The Transition from Turbulent to Laminar Gas Flow in a Heated Pipe," *Transactions of the ASME, Ser. C: Journal of Heat Transfer*, Vol. 92, No. 4, Nov. 1970, pp. 569–579.

[13] Coon, C. W. and Perkins, H. C., "Transition from the Turbulent to the Laminar Regime for Internal Convective Flow with Large Property Variations," *Transactions of the ASME, Ser. C: Journal of Heat Transfer*, Vol. 92, No. 3, Aug. 1970, pp. 506–512.

Rotational Stability of a Semielastic Body

JOHN R. GLAESE*

NASA George C. Marshall Space Flight Center, Huntsville, Ala.

IN this work we consider a system consisting of a flat plate elastically coupled to a rigid rod. This system is considered as an idealization of a rotating space station. We are interested in the effects of nonrigid coupling on the rotational stability of such systems and would like to see if there might be some advantage in using a flexible coupling between rigid parts as an aid in stabilizing a vehicle that would otherwise be unstable or in reducing the size of the control forces required and hence making a more economical system. We develop the linearized equations of motion and ascertain the stability of the linearized system as a function of the strength of the coupling for all configurations of the moments of inertia of the composite bodies. The most significant result of this work is the demonstration both mathematically and by a working model that rotation about the intermediate principal axis, which is unstable for rigid coupling, can be stabilized by weakening the coupling.

For purposes of this analysis, we assume the flat plate and rod are perfectly flat and straight, respectively, and that all motion takes place in free space. We define a body-fixed reference frame for the plate by fixing the origin at the center of mass with the z axis along the normal and x and y along the principal directions. The rod is coupled semielastically to the plate; i.e., it is joined in such a way that it can rotate in the x, z plane about the y axis and such that the equilibrium is

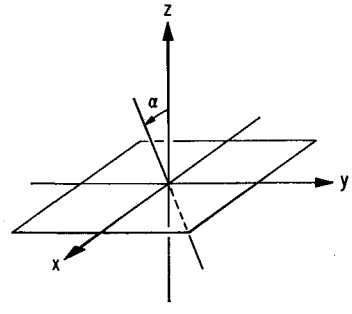

Fig. 1 Plate-fixed coordinate system.

Received November 9, 1970; revision received January 18, 1971.

* Presently on active duty with U.S. Army Corps of Engineers, assigned to the George C. Marshall Space Flight Center, NASA, Huntsville, Ala., in the Dynamics and Control Division, Aero-Astrodynamics Laboratory.

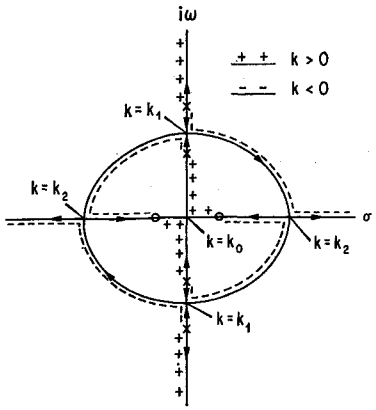

Fig. 2 Root locus, case 2, $I_1 < I_2 \leqq I_3$.

along z. The position of the rod relative to the plate is given by angle α (see Fig. 1). The inertia matrix for the plate is

$$\begin{bmatrix} I_1 & 0 & 0 \\ 0 & I_2 & 0 \\ 0 & 0 & I_1 + I_2 \end{bmatrix}$$

and in the same axes, the inertia matrix for the rod is

$$I_3 \begin{bmatrix} \cos^2\alpha & 0 & -\sin\alpha\cos\alpha \\ 0 & 1 & 0 \\ -\sin\alpha\cos\alpha & 0 & \sin^2\alpha \end{bmatrix}$$

If $\alpha = 0$ (rigid body limit), the combined inertia matrix is

$$\begin{bmatrix} I_1 + I_3 & 0 & 0 \\ 0 & I_2 + I_3 & 0 \\ 0 & 0 & I_1 + I_2 \end{bmatrix}$$

Thus, by properly selecting I_1, I_2, and I_3, any rigid body can be duplicated in its inertial properties. We assume a coupling minimum at $\alpha = 0$. Hence, to the lowest order, $V(\alpha) = \frac{1}{2}k\alpha^2$. The constant k here is a measure of the strength of the coupling with the body becoming rigid as $k \to \infty$. We shall allow k to take on either positive or negative values.

The treatment and results are summarized as follows. We linearize the equations about the equilibrium $\alpha = 0$ and the body rotating about the z axis at a spin rate Ω. The resulting equations are both homogeneous and time independent so that the solutions are of the form Ae^{st}, where A is the initial state vector. The stability of the linearized system can be determined from the values of the frequencies s, which are the solutions to the secular equation:

$$(s^2 + \Omega^2)\{I_2I_3(s^2 + \Omega^2)[(I_1 + I_3)s^2 + (I_3 - I_1)\Omega^2] + k[(I_1 + I_3)(I_2 + I_3)s^2 + (I_3 - I_1)(I_3 - I_2)\Omega^2]\} = 0$$

We see immediately that $s = \pm i\Omega$ are roots to this equation for all values of the system parameters. It is clear that these roots can correspond only to rigid body motion in which k can play no part. The quantity in braces is quadratic in s^2, and

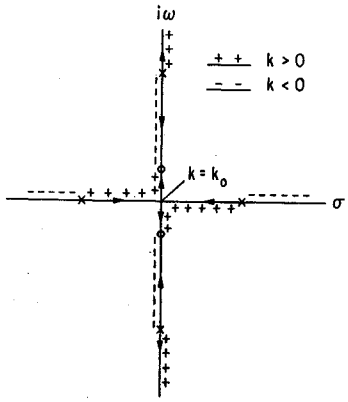

Fig. 3 Root locus, case 4, $I_1 < I_3$, $I_2 \leqq I_3$.

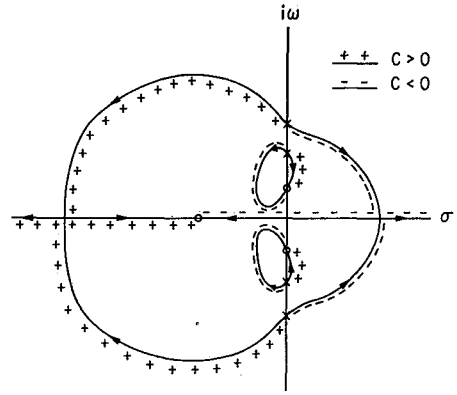

Fig. 4 Root locus, case 1 with damping.

hence the roots can be determined by quadratic formula; however, a more informative and more easily grasped analysis can be made using the root locus method. We need only the poles and zeroes of the root locus expression and these can be determined by inspection. The zeroes are

$$s = \pm i\Omega[(I_3 - I_1)(I_3 - I_2)/(I_3 + I_1)(I_3 + I_2)]^{1/2}$$

and the poles are

$$s = \pm i\Omega \text{ and } s = \pm i\Omega[(I_3 - I_1)/(I_3 + I_1)]^{1/2}$$

An analysis of these poles and zeroes reveals that there are four basic pole-zero configurations to consider. Case 1: $I_1 < I_3, I_2 < I_3$; Case 2: $I_1 < I_3 \leqq I_2$; Case 3: $I_2 \leqq I_3 < I_1$; and Case 4: $I_3 < I_1, I_3 < I_2$. There is an additional, degenerate case, $I_1 = I_3$, not covered by any of the previous. This case is unstable for all k because of the double root at $s = 0$ which allows solutions linear in time and hence, unbounded.

Let us treat the remaining cases in numerical order. The root loci are quite straightforward, and so we shall present explicit sketches only for cases 2 and 4, which are most interesting, being content to state the results for cases 1 and 3. Case 1 can be subdivided further into cases 1a and 1b. If

$$2I_3 > I_1 + 3I_2 + [(I_1 + 3I_2)^2 + 4I_1I_2]^{1/2}$$

case 1a obtains; otherwise, case 1b obtains. The values of k corresponding to the breakaway or departure points and the $s = 0$ root are

$$k_0 = I_2I_3\Omega^2/(I_2 - I_3)$$

$$k_2{}^1 = -2I_2I_3\Omega^2\{[I_2(I_3 - I_1)]^{1/2} \mp [I_3(I_1 + I_2)]^{1/2}\}^2/(I_1 + I_2)(I_2 + I_3)^2$$

These expressions are good for all cases, though k_1 and k_2 are meaningless if $I_3 < I_1$. Case 1a is stable whenever $k_0 < k < k_2$, $k_1 < k < 0$, $0 < k$. Case 1b is stable whenever $k_1 < k < 0$, $0 < k$. Case 1 corresponds to rotation about the axis of minimum moment inertia. Note that it is stable over a wide range of values of k including some negative values.

Case 2, corresponding to intermediate axis rotation, yields the most interesting result (see Fig. 2). Note that there are regions of stable rotations $k_1 < k < 0$, $0 < k < k_0$ and that, as $k \to \infty$; i.e., as the system tends toward a rigid body, the motion becomes unstable as expected.

Case 3 is also intermediate axis rotation, but now the system is unstable for all values of k. Since both cases 2 and 3 correspond to intermediate axis rotation, it is somewhat surprising that the results are so different. Cases 2 and 3 differ in that I_1 and I_2 are interchanged, which in effect changes the axis of rotation from the y axis to the x axis with the system otherwise unchanged. This shows the dependence of the stabilizing effect of elasticity on the axis of elasticity.

Finally, in case 4 (see Fig. 3), we treat rotation about the maximum and find, significantly, that the coupling must ex-

ceed a minimum strength for stability $k_0 < k$. This result agrees with rigid body results insofar as it is stable for large k.

Viscous damping in the rod-plate coupling can be treated in simple fashion. To include viscous damping in our equations, we replace k by $cs + k$ where c is the damping coefficient. The root locus expression can be written as $-1/k = G(s)$. With damping included this becomes $-1/cs + k) = G(s)$. If we let $k/c = m$, we can write $-1/c = (s + m)G(s)$. We can now treat m as a parameter and sketch the root loci for this expression. We shall give a representative sketch for case 1 treated previously for rotation about the minimum axis (see Fig. 4). The sketch in Fig. 4 assumes that $m > 0$; however, the general nature of the root locus remains the same as m is varied. It can be seen from Fig. 4 that the system is unstable for all c, and our previous discussion indicates that this is true for all m as well. Thus, this system is unstable for all values of c ($c \neq 0$) and all values of k. By similar investigations, the other cases except case 4 are found to be unstable regardless of the sign of the damping constant. Damping is destabilizing in case 4 for negative damping but stabilizing if $c > 0$. That damping is destabilizing for all but major axis rotation is to be expected, but that negative damping is not stabilizing about the minimum axis is contrary to what one might expect from energy considerations. We can treat viscous damping in all coordinates for small damping constants by noting the displacement of the poles and zeroes. With this technique, we can show that small damping forces of appropriate signs and relative magnitudes can make the system asymptotically stable.

The results we have obtained are based on an analysis of the linearized equations of motion of the physical system. Asymptotic stability of the linearized system is sufficient for asymptotic stability of the motion, but simple stability is not sufficient for stability of motion. It is necessary, however, and the fact that the linear motion is stable means that, though the system may not be stable, the drift away from equilibrium takes place relatively slowly so that stability could be achieved by implementing a control system which employs small control forces. As an example, suppose that by reason of external constraints it became necessary to maintain rotation about the intermediate axis. Clearly, the system employing the semielastic scheme could be controlled by a much smaller and hence lighter system.

To demonstrate our results, we devised a simple free-fall experiment, using a model constructed from cardboard and scotch tape, and the use of paper clips as counterweights to provide the desired moments of inertia. The scotch tape not only held the two moving parts together but provided the elasticity. By addition of bracing supports we were able to make the coupling variable from elastic to rigid without requiring a change in the distribution of mass. We arranged the masses so that the moments of inertia were configured as in case 2 (intermediate axis rotation). At first the coupling was made rigid. As expected, when the model was tossed spinning into the air, it began to tumble wildly after less than a second of flight. This was repeated several times with similar results each time. This result was not surprising since we know a rigid body is unstable about its intermediate axis. Next we relaxed the coupling so that it was no longer rigid. This time when the model was tossed spinning into the air, there was no tumbling, and the model continued to spin smoothly throughout its flight, dramatically demonstrating the effect.

We have shown that motion about the intermediate axis can be made stable for a body structured like a dually rotating space station might be and that it could be advantageous to make the coupling between spun and despun parts elastic in order to enhance the controllability of such a vehicle. This investigation was conducted in order to explore some of the problems of rotating space stations in Earth orbit and their possible solutions. The author is not aware of any other work along this line having been done.

Experimental Results on Crosshatched Ablation Patterns

HANS W. STOCK* AND JEAN J. GINOUX†
von Kármán Institute for Fluid Dynamics, Rhode-Saint-Genèse, Belgium

DURING recent years surface patterns created during ablation on re-entry or wind-tunnel models have been the subject of considerable interest. They appeared in form of streamwise striations, turbulent wedges and criss-crossed grooves. Among these, the latter has been studied the most intensively. Experimental results on patterns parameters are given in Ref. 1, 2, and 3. Although attempts have been made trying to explain the triggering mechanism[2–6] of the phenomenon, the problem is not yet solved.

In this Note, the results of an experimental program on crosshatching are presented.

1. Test Facility

Tests were made at a freestream Mach number of 5.3 with the following tunnel stagnation conditions

$$T_{ST} = 150\text{–}400°\text{C}$$

$$P_{ST} = 12\text{–}32\ \text{kgf/cm}^2$$

giving unit freestream Reynolds numbers of

$$1.3\text{–}3.8 \times 10^7/\text{m}$$

2. Models

The 10 to 50° total vertex angle cones and the 10° cones with 12 to 40° total flares were tested at zero angle of attack. Typical test results are shown in Fig. 1. The models had pointed steel noses and a maximum basic diameter of 8 cm.

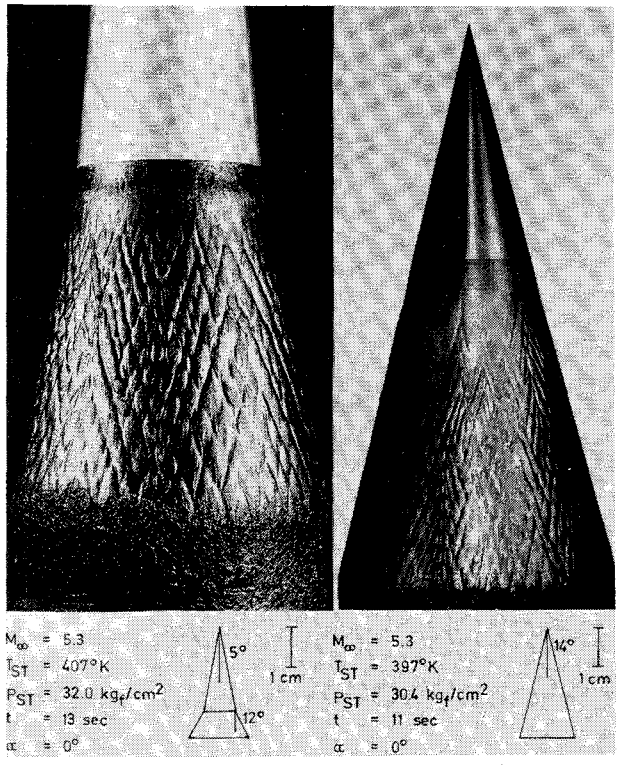

Fig. 1 Typical test results on wax models.

Received October 16, 1970.

* Research Assistant.
† Professor, Brussels University and Head of VKI Department of Supersonics and Hypersonics.